Power-law rheology and the dynamical heterogeneity in a sheared granular material

Takahiro Hatano
Earthquake Research Institute, University of Tokyo, 1-1-1 Yayoi, Bunkyo, Tokyo 113-0032, Japan
(Dated: November 11, 2008)

Rheology of a granular material at the jamming density is investigated using molecular dynamics simulation. It is found that shear stress exhibits power-law dependence on shear rate with a nontrivial exponent. Due to the criticality of the jamming transition point, finite-size effect is observed in smaller systems at lower shear rates. Finite-size scaling indicates the correlation length algebraically diverges in the zero shear rate limit. It is also found that the dynamical susceptibility monotonically decreases with time so that the dynamical heterogeneity is detected by a two-point correlation function. Several exponents that describe rheology, the correlation length, and the amplitude of the dynamical susceptibility are estimated.

Consider an assembly of repulsive particles at zero temperature, the density of which is so low that there is no contact between particles. By increasing density, the particles are inevitably in contact above a certain density and the system obtains rigidity without crystallization [1, 2]. This phenomenon and the threshold density are now referred to as the jamming transition and the jamming density, respectively. It is believed that the jamming transition point, which is also referred to as *point J*, is a critical point at zero temperature due to several evidences: finite-size scaling of the transition point [2], and the growing correlation length and relaxation time [3, 4, 5, 6, 7, 8, 9]. However, in contrast to conventional critical phenomena, these length and time scales are apparent only through dynamic quantities such as the displacement of particles in a certain lag time. Quite interestingly, this dynamic critical fluctuation is originally observed in supercooled liquids [10, 11], and is referred to as the dynamical heterogeneity. Recalling that the jamming transition is the solidification without crystallization, the jamming and glass transitions might be closely related.

However, the nature of point J is still opaque because the critical exponents and the mechanism that yields the dynamical heterogeneity are not clear. As regards the critical exponents, it is generally accepted that $\xi \sim |\phi_J - \phi|^{-\nu}$, where ϕ and ϕ_J denote the density of a system and the jamming density. The critical exponent ν is estimated as 0.6 ± 0.1 [3, 6, 8, 9, 12]. However, the exponents for other relevant variables are not known. For example, because point J is defined at zero temperature and zero shear rate limit [1, 13], temperature T and shear rate γ are also relevant variables so that the correlation length must diverge as $T \to 0$ and $\gamma \to 0$. However, we still do not know the nature of divergence; i.e., power law, Vogel-Fulcher law, etc. Unfortunately, the concept of temperature in granular media is not generally established at this point so that we focus only on shear rate.

In this paper, by molecular dynamics simulation, we investigate rheology of a granular material at the jamming density focusing on the particle dynamics and the correlation length. Several exponents that describe rheology, the correlation length, and the amplitude of the dynamical susceptibility are estimated.

Our simulation system consists of monodisperse spheres, the diameter of which is denoted by d. The repulsive force between particles is given as $k(d - |\mathbf{r}|)$ if $d > |\mathbf{r}|$ and otherwise zero, where $\mathbf{r}$ denote the relative vector of the position of two particles. The inelasticity is modeled by $(\zeta \mathbf{n} \cdot \dot{\mathbf{r}})\mathbf{n}$, where $\mathbf{n} = \mathbf{r}/|\mathbf{r}|$. The total interaction is the sum of the above two terms. Throughout this study, we adopt the units in which $d = 1$, $k = 1$, and $m = 1$, where m is the mass of a particle. We set $\zeta = 2$, which corresponds to the damping limit; i.e., the coefficient of restitution is zero.

The dimensions of the system is $L \times L \times L$, where L is varied from 3.45 to 40.32. Here we fix the density of the system to be 0.639 in the volume density, which is considered as the jamming density for three dimensional systems with the precision of ± 0.001. The largest system ($L = 40.32$) contains 80,000 particles, while the smallest system consists of only 50 particles. We set the flow direction along the y axis and the velocity gradient along the z axis, and adopt Lees-Edwards boundary conditions [14]. The equations of motion are given by SLLOD equations;

$$\dot{\mathbf{q}}_i = \frac{\mathbf{p}_i}{m} + \gamma q_{z,i} \mathbf{n}_y, \tag{1}$$

$$\dot{\mathbf{p}}_i = \mathbf{F}_{\rm int} - \gamma p_{z,i} \mathbf{n}_y, \tag{2}$$

where $\mathbf{F}_{\rm int}$ denotes the repulsive interaction force between particles and $\mathbf{n}_y$ is the unit vector along the y axis. In the present configuration, the control parameters are the shear rate γ and the system size L so that the shear stress S and the pressure P are formally expressed as $S = S(\gamma, L^{-1})$ and $P = P(\gamma, L^{-1})$.

First we discuss power-law rheology shown in FIG. 1. In the higher shear rate region, the pressure and the shear stress exhibit power-law dependence on shear rate, each of which has different exponents: $S \propto \gamma^{1/\delta_S}$ and $P \propto \gamma^{1/\delta_P}$, where $1/\delta_S = 0.64 \pm 0.02$ and $1/\delta_P = 0.49 \pm 0.01$. Note that these exponents differ from 2.0 (i.e., Bagnold's scaling [15]), which is valid only in unjammed regime

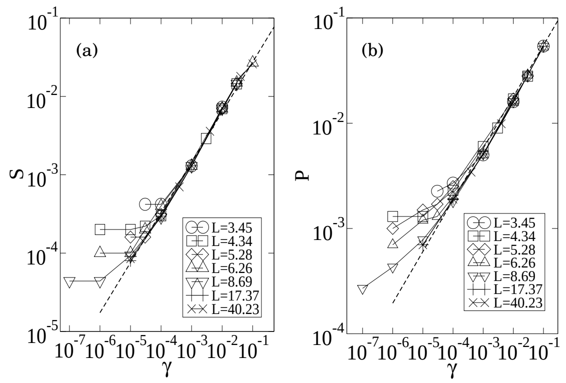

FIG. 1: System-size dependence of the rheological properties. (a) Shear-rate dependence of shear stress. The dashed line denotes $S \propto \gamma^{0.64}$. (b) Shear-rate dependence of pressure. The dashed line denotes $P \propto \gamma^{0.5}$.

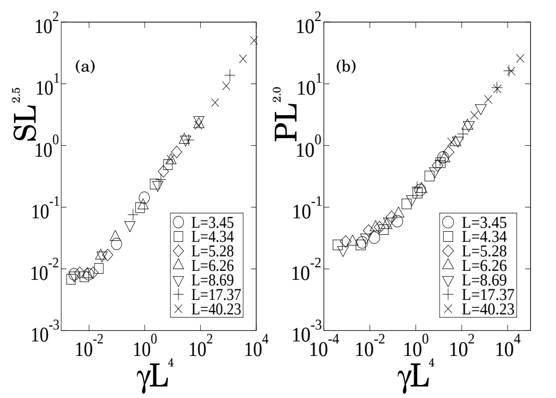

FIG. 2: Collapse of the rheological data shown in FIG. 1 by finite-size scaling: (a) Eq. (3), and (b) Eq. (4).

where the stiffness of the particles does not affect the mean free time. Note that this power-law rheology with nontrivial exponent is one of the evidences of the criticality of point J. We also remark that these exponents do not contradict those previously conjectured [16, 17].

These power-law behaviors, however, do not hold in the lower shear rate region and there exists crossover. Moreover, the shear rate at which the crossover occurs depends on the system size; it shifts lower as the system becomes larger. Indeed, this crossover is described by finite-size scaling laws, which are of the same form as those in conventional critical phenomena [18].

$$S(\gamma, L) = L^{-1/y_S} f_S(\gamma L^{1/y_\gamma}), \tag{3}$$
$$P(\gamma, L) = L^{-1/y_P} f_P(\gamma L^{1/y_\gamma}), \tag{4}$$

where f_S and f_P are scaling functions. FIG. 2 shows the collapse of the rheological data using Eqs. (3) and (4), where the exponents are estimated as $1/y_S = 2.5 \pm 0.2$, $1/y_P = 2.0 \pm 0.2$, and $1/y_\gamma = 4.0 \pm 0.5$.

We remark three important properties that are deduced from Eqs. (3) and (4). First, the exponents for power-law rheology, δ_S and δ_P, are expressed by y_γ, y_S, and y_P. Because the rheology does not depend on the system size in the thermodynamic limit $L \to \infty$, the scaling functions must behave as $f_S(z) \propto z^{y_\gamma/y_S}$ and $f_P(z) \propto z^{y_\gamma/y_P}$, respectively. They lead to $S(\gamma, \infty) \propto \gamma^{y_\gamma/y_S}$ and $P(\gamma, \infty) \propto \gamma^{y_\gamma/y_P}$. We thus obtain equalities for the exponents, $1/\delta_S = y_\gamma/y_S$ and $1/\delta_P = y_\gamma/y_P$, which are confirmed by inserting the above values. Second, because finite-size crossover occurs at $L/\gamma^{-y_\gamma} \sim 1$, we can expect that there exist the growing correlation length that depends on the shear rate as

$$\xi(\gamma) \sim \gamma^{-y_\gamma}, \tag{5}$$

where $y_\gamma = 0.25 \pm 0.03$. We show that, in the following paragraph, this growing correlation length is explicitly observed in a spatial correlation function. Third, inserting $L = \xi$ into Eqs. (3) and (4), we obtain $S \sim \xi^{-1/y_S}$ and $P \sim \xi^{-1/y_P}$, which represents the scaling dimensions of the shear stress and the pressure, respectively.

From Eq. (5), it is expected that the dynamical heterogeneity is enhanced in the $\gamma \to 0$ limit. In order to detect the dynamical heterogeneity, we define the four-point correlation function $h(\mathbf{r}, \tau) \equiv \langle h_t(\mathbf{r}, \tau) \rangle_t$, where

$$h_t(\mathbf{r}, \tau) \equiv \frac{1}{N} \sum_{i,j} \delta m_i(\tau; t) \delta m_j(\tau; t) \delta(\mathbf{r} - \mathbf{x}_i(t) + \mathbf{x}_j(t)). \tag{6}$$

Here $\delta m_i(\tau; t) \equiv m_i(\tau; t) - \langle m_i(\tau; t) \rangle_i$, where

$$m_i(\tau; t) \equiv \exp\left[-\left(\frac{\delta x_i(\tau; t)}{\langle \delta x_i(\tau; t) \rangle_i} \right)^2 \right], \tag{7}$$
$$\delta x_i(\tau; t) = \left| \int_t^{t+\tau} ds \frac{\mathbf{p}_i(s)}{m} \right|. \tag{8}$$

Using $h(\mathbf{r}, \tau)$, we introduce the dynamical susceptibility $\chi_4(\tau) \equiv \int d\mathbf{r} h(\mathbf{r}, \tau)$. As is shown in FIG. 3. the amplitude of $\chi_4(\tau)$ can be scaled by $A(\gamma)$, which is proportional to γ^{-c}. The exponent is estimated as $c = 0.65 \pm 0.05$. More importantly, this dynamical susceptibility seems to be a monotonically decreasing function with the lag time τ. This means that the dynamical heterogeneity can be detected in the $\tau \to 0$ limit; i.e., two-point correlation of the instantaneous velocity field. This makes an apparent contrast to supercooled liquids and vibrated granular matters, in which the dynamical susceptibility reaches maximum after a considerable lag time. This is because the particles are continuously rearranged due to externally applied shear so that the agitation without structural relaxation is absent in the present system. In addition, the thermal motion of particles, which predominates the structural relaxation, is absent in granular matters. (In particular, the coefficient of restitution is zero in the present system.) Due to these points, the instantaneous velocity leads to structural relaxation.

In the rest of this paper, we thus investigate the nature of the instantaneous velocity field. Figure 4 shows the

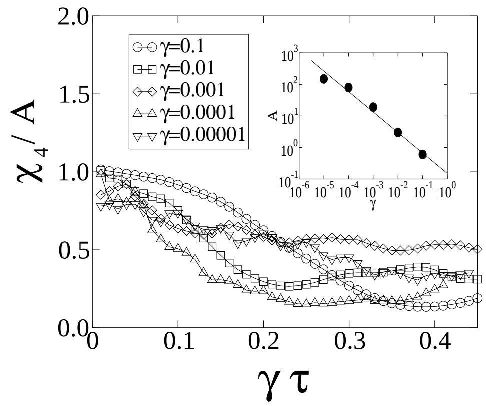

FIG. 3: The temporal behavior of the dynamical susceptibility $\chi_4(\tau)$. The lag time τ is multiplied by the shear rate γ so that the horizontal axis represents strain. Note that the dynamical susceptibility $\chi_4(\tau)$ is normalized by $A(\gamma)$. (Inset) The amplitude $A(\gamma)$ is proportional to $\gamma^{-0.65}$, shown as the solid line.

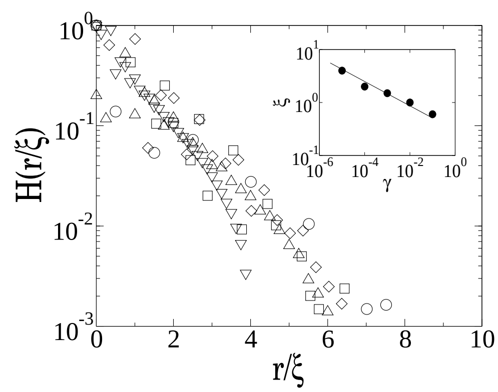

FIG. 4: The correlation function defined by Eqs. (6) and (9). The legends are the same as those in FIG. 3. Note that the length scale is normalized by ξ. (Inset) The correlation length ξ is proportional to $\gamma^{-0.23}$, shown as the solid line.

two-point correlation function defined in the $\tau \to 0$ limit of Eq. (6).

$$H(r) \equiv \frac{1}{g(r)h(0,0)} \int d\mathbf{\Omega} h(\mathbf{r},0), \tag{9}$$

where $g(r)$ denotes the radial distribution function and $\mathbf{\Omega}$ denotes the solid angle. This correlation function clearly shows that the correlation length ξ is proportional to γ^{-y_γ}, where $y_\gamma = 0.23 \pm 0.02$. Note that this is consistent with Eq. (5), which results from finite-size scaling. Therefore we can conclude that the finite-size effect in rheology occurs as the correlation length is comparable to the system size.

Note that $H(r)$ defined by Eqs. (6) and (9) characterizes the spatial heterogeneity of mobility, but does not have information on the specific motion of the particles of high mobility. In the kinetic theoretical point of view, it is important to know how particles rearrange cooperatively in a marginally-jammed system. To this end, we define a spatial correlation function for the instantaneous velocity vectors;

$$G(\mathbf{r},t) \equiv \frac{1}{N} \sum_{i,j} \mathbf{p}_i(t) \cdot \mathbf{p}_j(t) \delta(\mathbf{r} - \mathbf{x}_i(t) + \mathbf{x}_j(t)|). \tag{10}$$

This characterizes the spatial correlation of co-moving particles, such as ring collision in a dilute gas [20] and the stringlike cooperative motion (SCM) in glassy systems [7, 19]. In addition, note that particles with larger velocity predominate $G(\mathbf{r},t)$, because the magnitude of velocity is taken into account in Eq. (10). Here we average the correlation function with respect to time $G(\mathbf{r}) \equiv \langle G(\mathbf{r},t)\rangle_t$, and the solid-angle dependence is integrated out as is done in Eq. (9). After this procedure, the correlation function $G(r)$ becomes an exponentially decaying function so that it can be scaled by a length scale λ, which should be interpreted as the characteristic length of SCM. The scaled correlation function is shown in FIG. 5. The characteristic length of SCM increases as the shear rate decreases as is shown in the inset of FIG. 5. The exponent is estimated as 0.15 if we assume power law; i.e., $\lambda \sim \gamma^{-0.15}$. This is to be compared with Eq. (5), from which we can conclude that SCM is not directly related to the dynamical heterogeneity. This situation is similar in two-dimensional air-fluidized beads [7], in which several characteristic lengths for SCM are found. The kinetics of the dynamical heterogeneity is thus still open.

The discussions so far constitute the main results of this study. In the following, we remark two points that are peripherally related to the main results. The first point is the comparison of the present result with Ref. [9], in which a scaling law for the correlation length is found for a two-dimensional overdamp system. This implies that the correlation length diverges as $\xi \propto S^{-0.5}$.

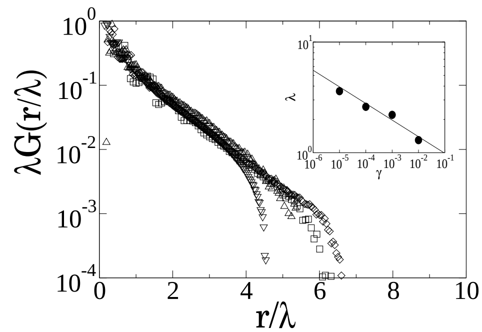

FIG. 5: The correlation function defined by Eq. (10), which represents the extent of stringlike cooperative motion. Note that the length scale is normalized by the characteristic length λ. The legends are the same as those in FIG. 3. (Inset) The characteristic length $\lambda(\gamma)$ is proportional to $\gamma^{-0.15}$, shown as the solid line.

TABLE I: The exponents estimated in the present study.

Observable	Shear stress		Pressure		Length	Susceptibility
Critical	$1/y_S$	$1/\delta_S$	$1/y_P$	$1/\delta_P$	y_γ	c
exponents	2.5(2)	0.64(2)	2.0(2)	0.49(1)	0.23(2)	0.65(5)

Because they obtain $S \propto \gamma^{0.42}$ at the critical density, this leads to $\xi \sim \gamma^{-0.21}$. The latter is consistent to the present result, while the former is different. The reason for this discrepancy is not due to the dimensionality but the artificial overdamp (massless) dynamics in Ref. [9], because we obtain $S \propto \gamma^{0.64}$ in a two-dimensional granular system and also $S \propto \gamma^{0.42}$ in a three-dimensional overdamp system, the details of which are to be presented elsewhere.

Then we wish to remark the experimental validation of Eq. (5) with $y_\gamma \sim 0.25$. Although this exponent is so small that the correlation length shown in FIG. 4 does not significantly increase (by approximately one decade), it is observed to increase by two order of magnitudes in an experiment [21].

In summary, power-law rheology is found in a granular material at the jamming density. Finite-size scalings of power-law rheology indicate the diverging correlation length in the zero shear rate limit. The dynamical susceptibility becomes maximum for instantaneous velocity so that the correlation length of the dynamical heterogeneity is defined by a two-point correlation function. This correlation length directly supports the result of finite-size scaling. Various critical exponents are estimated, as summarized in Table. I.

[1] C. S. O'Hern, S. A. Langer, A. J. Liu, and S. R. Nagel, Phys. Rev. Lett. **88**, 075507 (2002)

[2] C. S. O'Hern, L. E. Silbert, A. J. Liu, and S. R. Nagel, Phys. Rev. E **68**, 011306 (2003).

[3] J. A. Drocco, M. B. Hastings, C. J. Olson Reichhardt, and C. Reichhardt, Phys. Rev. Lett. **95**, 088001 (2005).

[4] O. Dauchot, G. Marty, and G. Biroli, Phys. Rev. Lett. **95**, 265701 (2005).

[5] A. R. Abate and D. J. Durian, Phys. Rev. E **74**, 031308 (2006).

[6] A. R. Abate and D. J. Durian, Phys. Rev. E **76**, 021306 (2007).

[7] A. S. Keys, A. R. Abate, S. C. Glotzer, and D. J. Durian, Nature Phys. **3**, 260 (2007).

[8] F. Lechenault, O. Dauchot, G. Biroli, and J.-P. Bouchaud, Europhys. Lett. **83**, 46003 (2008).

[9] P. Olsson and S. Teitel, Phys. Rev. Lett. 99, 178001 (2007).

[10] W. Kob, C. Donati, S. J. Plimpton, P. H. Poole, and S. C. Glotzer, Phys. Rev. Lett. **79**, 2827 (1997).

[11] R. Yamamoto and A. Onuki, Phys. Rev. Lett. **81**, 4915 (1998); Phys. Rev. E **58**, 3515 (1998).

[12] M. Wyart, L. E. Silbert, S. R. Nagel, and T. A. Witten, Phys. Rev. E **72**, 051306 (2005).

[13] A. J. Liu and S. Nagel, Nature (London) **396**, 21 (1998).

[14] M.P. Allen and D.J. Tildesley, *Computer Simulation of Liquids*, (Clarendon, Oxford, 1989).

[15] See, for example, L. E. Silbert, D. Ertas, G. S. Grest, T. C. Halsey, D. Levine, and S. J. Plimpton, Phys. Rev. E **64**, 051302 (2001); N. Mitarai and H. Nakanishi, Phys. Rev. Lett. **94**, 128001 (2005), and references therein.

[16] T. Hatano, J. Phys. Soc. Jpn., in press (2008).

[17] T. Hatano, M. Otsuki, and S. Sasa, J. Phys. Soc. Jpn, **76**, 023001 (2007).

[18] In general, finite-size scaling reads $S(\Phi, \gamma, L) = L^{-1/y_S} f_S(\Phi L^{1/y_\Phi}, \gamma L^{1/y_\gamma})$. where Φ is the distance from the critical density. Thus, Φ must be zero (or $\Phi L^{1/y_\Phi} \simeq 0$) if one wishes to estimate y_γ.

[19] C. Donati, J. F. Douglas, W. Kob, S. J. Plimpton, P. H. Poole, and S. C. Glotzer, Phys. Rev. Lett. **80**, 2338 (1998).

[20] K. Kawasaki and I. Oppenheim, Phys. Rev. A **139**, 1763 (1965).

[21] H. Katsuragi, A. Abate, and D. J. Durian (private communication).